Vol. 255: 43–54, 2003 | MARINE ECOLOGY PROGRESS SERIES
Mar Ecol Prog Ser | Published June 24

Partitioning of physical and biogeochemical contributions to short-term variability of pCO_2 in a coastal upwelling system: a quantitative approach

J. Gago*, X. A. Álvarez-Salgado, F. F. Pérez, A. F. Ríos

CSIC, Instituto de Investigacións Mariñas, Eduardo Cabello 6, 36208 Vigo, Spain

ABSTRACT: A considerable body of literature has addressed the role that coastal upwelling systems may play in global processes, especially in the ocean carbon cycle. It is often difficult to separate the effects of physical and biogeochemical processes on the partial pressure of carbon dioxide (pCO_2) in coastal upwelling systems due to the tight coupling between these processes. In this work we propose a novel approach to quantify physical (advection and diffusion of inorganic carbon species, *in situ* warming) and biogeochemical (production and consumption of inorganic carbon species) effects on surface pCO_2 using an inverse method. It is applied to the Ría de Vigo, a large coastal indentation in the NW Iberian shelf. Physical and biogeochemical processes affecting surface pCO_2 variability are quantified during spring, summer, autumn and winter. Our results show the dominance of vertical advection, turbulent diffusion and net ecosystem production of organic carbon (ΔC_{org}) components over other processes (calcification and surface warming) on a short timescale (2 to 4 d). The study reveals that physical transport of inorganic carbon species explains ~50% of the observed pCO_2 variability and ΔC_{org} accounts for most of the remaining 50%.

KEY WORDS: pCO_2 · Carbon cycle · Inversebox–methods · Coastal upwelling · Galician rías · NW Spain

INTRODUCTION

Increased atmospheric levels of carbon dioxide (CO_2) account for about 60% of the CO_2 emitted by fossil fuel burning and cement making. The oceans and terrestrial systems absorb the remainder of these emissions (Houghton et al. 1996). Net CO_2 uptake by the oceans ranges from 17 to 39% of the fossil fuel emissions (e.g. Siegenthaler & Sarmiento 1993, Schimel et al. 1996). The direction of the air-sea CO_2 exchange is determined ultimately by the difference of CO_2 pressure (pCO_2) between the atmosphere and surface seawater. Atmospheric pCO_2 is relatively constant and is calculated from data measured at stations around the world (Komhyr et al. 1985). On the other hand, seawater pCO_2 varies significantly, both temporally and spatially, as a result of a superposition of physical and biogeochemical factors (e.g. Takahashi et al. 1993). Organic carbon production (photosynthetic CO_2 fixation) and consumption (respiratory release of CO_2) influence the oceanic CO_2 system by respectively decreasing or increasing seawater pCO_2. Calcification produces a net increase of pCO_2, whereas $CaCO_3$ dissolution provokes a decrease. Temperature and freshwater cycles also influence seawater pCO_2 values. Temperature affects the acid constants of the CO_2 system and its solubility in seawater: an increase of 1°C provokes an increase of 4.23% in pCO_2 (Takahashi et al. 1993). The effect of the freshwater cycle on surface pCO_2 also involves the acid constants and the solubility of CO_2 in seawater, apart from the highly variable inorganic carbon content of rivers.

Continental shelves and slopes usually have high primary production rates and enhanced water flows that results in intensified gradients of biogeochemical parameters (Walsh 1991, Wollast 1993). These processes affect seawater pCO_2 in several ways and, therefore, the air-sea exchange of CO_2. Coastal areas

*Email: gago@iim.csic.es

affected by wind-driven upwelling are relevant for the global carbon cycle because of their enhanced physical and biological activity compared with other environments. Equatorial and coastal upwelling systems account for 5 to 15% of the new production of the world's oceans (Knauer 1993).

A question has been recurrently addressed about the role of upwelling systems in the global carbon cycle: Do they act as a net sinks or sources of CO_2 to the atmosphere? (e.g. Watson 1995). We try to clarify this question by separating the physical and biogeochemical components of seawater pCO_2 with a quantitative approach based on the combination of relevant carbon rates and water fluxes derived with an inverse method and a first-order removal mechanism for salinity, temperature, total inorganic carbon content (C_T) and total alkalinity (A_T).

Despite the fact that inorganic carbon dynamics in coastal upwelling areas have previously been reported — e.g. by Copin-Montegut & Raimbault (1994) in Perú, Torres et al. (1999) in Chile, Borges & Frankignoulle (2002) and Gago et al. (2003) in NW Iberia — this study is one of the first attempts to quantify the relative contribution of physical (advection and diffusion of inorganic carbon species, *in situ* warming) and biogeochemical (production and consumption of inorganic carbon species) processes to the variability of surface pCO_2 on a time scale of 2 to 4 d. Previous studies have established that this is the most suitable sampling frequency to study the coupling between meteorological forcing and hydrography in the NW Iberian margin (Álvarez-Salgado et al. 1993).

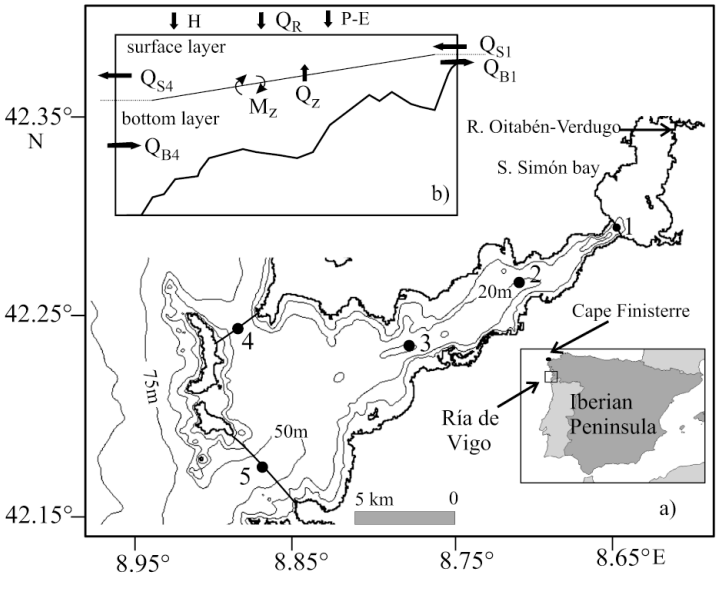

Fig. 1. (a) Chart of survey area (Ría de Vigo, NW Iberian upwelling system), showing 5 sampling sites (●) distributed along the embayment. Inner (Stn 1) and outer (Stns 4 and 5) boundaries delimit the study area; meteorological observatory at Cape Finisterre is indicated. Isobaths of –20, –50 and –75 m are shown. (b) Box geometry of the system. $Q_R + P - E$: hydrological balance (Q_R = river runoff, P = precipitation and E = evaporation); Q_B and Q_S: surface and bottom horizontal advective fluxes; Q_Z and M_Z: vertical advective and mixing fluxes, respectively; H: heat exchange across the sea surface. Subscripts 1 and 4 refer to the inner and outer boundary, respectively

MATERIALS AND METHODS

Sampling. The study site is the coastal upwelling system of the Ría de Vigo, one of the 4 large, flooded tectonic valleys located in NW Spain (Fig. 1). Wind-driven upwelling occurs there from April–May to September–October (upwelling season) and provokes an enhanced positive circulation pattern (Wooster et al. 1976). The rest of the year (downwelling season) is characterized by southerly winds that frequently produce a reversal of positive circulation (Álvarez-Salgado et al. 2000), with the ría circulation similar to that of a negative estuary. The Ría de Vigo is a large embayment (2.76 km^3) with a unique open-boundary, whereby the typical 3-dimensional water transport over open shelves is reduced to 2 dimensions because of negligible along-shore transport (Gilcoto et al. 2001).

Intensive hydrographic sampling was performed in the Ría de Vigo during 4 contrasting periods in 1997: 7 to 23 April (spring), 1 to 18 July (summer), 15 September to 2 October (autumn), and 1 to 11 December (winter). There were 5 sampling stations, 4 along the main axis of the embayment and 1 at the shallower entrance, north of the Isles Cies (Fig. 1). Full-depth continuous conductivity-temperature-depth profiles were recorded at each sampling site with a SBE 25 CTD device. Conductivity measurements were converted into practical salinity-scale values (UNESCO 1986). Subsequently, seawater samples for pH and A_T determination were collected from 3 to 5 depths with 5 l Niskin bottles. This procedure was repeated every 2 to 4 d during each of the 4 sampling periods. A total of 22 surveys were performed: 6 during spring, summer and autumn, and 4 during the winter period. pH was measured potentiometrically (Pérez & Fraga 1987a). A_T was determined by 1 end-point potentiometric titration (Pérez & Fraga 1987b). The electrodes were calibrated to the National Bureau of Standards (US) scale. The accuracy of pH and A_T measurements was ±0.002 and 1.4 µmol kg^{-1}, respectively, as determined using samples of Batches 33, 35 and 37 of the certified reference material (CRM) provided by Dr. A. Dickson, University of California. C_T and pCO_2 were calculated from pH and A_T using the carbonic acid constants of Mehrbach et al. (1973) and the solubility constant of

Weiss (1974). The accuracy of pH and A_T measurements produces an estimated error of ±3 µmol kg^{-1} and 3 µatm for calculated C_T and pCO_2, respectively. The CO_2 fluxes across the air-seawater interface were taken from Gago et al. (2003). Finally, offshore Ekman transport was calculated for Cape Finisterre (Fig. 1) according to Wooster et al. (1976).

Partitioning of physical and biogeochemical components using an inverse-box method. The study system is delimited by 2 boundaries (Fig. 1). The inner boundary separates the ría from San Simón Bay, the estuary of the river Oitabén-Verdugo; the outer boundary separates the ría from the continental shelf. The geometry of the Ría de Vigo (surface and cross-sectional areas and volume) was obtained from accurate charts published by the Spanish 'Instituto Hidrográfico de la Marina'. The study system is divided into 2 layers (surface and bottom), flowing in opposite directions; the thin stratum of water between the surface and bottom layer with no horizontal motion constitutes the gravity center. Average salinity and temperature of the surface and bottom layers at each boundary were obtained by simple numeric integration of the CTD profiles. Average concentrations of C_T and A_T in the surface and bottom layer at each boundary and in the box (volume of water considered) were calculated from C_T and A_T data from 3 to 5 discrete samples. Continental runoff to the Ría de Vigo (Q_R) was estimated according to Ríos et al. (1992) from precipitation in the drainage basin.

To quantify the net effect of physical and biogeochemical processes on the pCO_2 of the surface layer of the ría, a first-order removal mechanism for salinity, temperature, C_T and A_T was assumed. This approach has long been used to study the fate of chemicals dissolved in marine systems (see Martin et al. 1986 for a complete review on this topic), and we apply it here to the study of short-term variability of inorganic carbon species. With regard to net input to and output from the surface layer, the temporal changes in thermohaline and chemical variables between 2 consecutive surveys for a situation of upwelling can be expressed as:

$$\frac{\Delta(C\times V)}{\Delta t} = \overline{F} + Q_{S1}\times C_{S1} + Q_Z\times C_Z + M_Z\times C_L + Q_R\times C_R - Q_{S4}\times\frac{C_{S4}}{C}\times C - M_Z\times C + \overline{\mathrm{NEB}} \quad (1)$$

where C is average salinity, temperature, C_T or A_T in the box between 2 consecutive surveys. In this way, outflux is proportional to the value of C in the upper layer. The term $\overline{F}$ accounts for the air-sea exchange of CO_2 ($\overline{F}CO_2$) in the case of C_T and heat ($\overline{H}$) in the case of temperature; $\overline{H}$ was estimated by Álvarez-Salgado et al. (2000) for the 1997 surveys. Subscripts 1 and 4 refer to the inner and outer boundaries of the ría, respectively (Fig. 1); subscripts L, Z and R represent bottom layer, level of no motion and river runoff, respectively (see Table 1). The term $<C_{S4}>/<C>$, the ratio of average C concentrations in the outer boundary and the box between 2 consecutive surveys, is introduced to correct the lack of homogeneity of the surface layer of the ría (~1.2 km^3).

Water flow (Q_S, Q_Z, Q_R and M_Z, see Fig. 1 and Table 1 for definitions) for the 1997 surveys had already been obtained by Álvarez-Salgado et al. (2000) using a multiparameter inverse method. Data on water flow and the average concentrations of the different inorganic carbon species in the upper and lower layers, allows calculation of salinity, temperature, C_T and A_T convective and diffusive fluxes. $\overline{\mathrm{NEB}}$ represents the net ecosystem budget of C (salinity, temperature, C_T or A_T). For salinity and temperature, $\overline{\mathrm{NEB}} = 0$; for C_T, $\overline{\mathrm{NEB}} = -\Delta C_{org} - \Delta CaCO_3$, where ΔC_{org} and $\Delta CaCO_3$ are the net ecosystem production of organic carbon and calcium carbonate, respectively. According to Broecker & Peng (1982), the $\overline{\mathrm{NEB}}$ of A_T equals – $\overline{\mathrm{NEB}}$ of nitrate (= $[^{16}_{106}] \times \Delta C_{org}$) in the case of phytoplankton organic carbon, and equals $-2\times\Delta CaCO_3$ in the case of calcium carbonate. Therefore, the $\overline{\mathrm{NEB}}$ of A_T is equal to $(^{106}/_{16}) \times \Delta C_{org} - 2\times\Delta CaCO_3$. Integration of Eq. (1) between 2 consecutive surveys yields:

$$C_2 = C_1\times e^{-B\times\Delta t} + \left(\frac{A}{B}\right)\times(1-e^{-B\times\Delta t}) + \left(\frac{\overline{\mathrm{NEB}}}{B}\right)\times(1-e^{-B\times\Delta t}) \quad (2)$$

where $\Delta t = t_2 - t_1$. Table 2 shows the equations that describe A and B for upwelling and downwelling conditions. During upwelling, surface water flows are directed toward the shelf because northerly winds enhance the positive estuarine circulation pattern. During downwelling conditions, circulation results from the balance between the intensity of southerly winds (which tend to introduce shelf waters into the ría) and river runoff (which tends to release continental waters onto the shelf). In general, there is an oceanic surface water inflow to the ría that returns to the shelf through the bottom layer and a surface flow from San Simón Bay to the ría from river runoff.

A/B is the expected value of C in the surface layer of the ría arising from the physical transport of C to the system; B is equivalent to the inverse of the flushing rate ($B \sim {}^1/_{tr}$, d^{-1}) of the surface layer of the ría, and the term $1/B \times (1 - e^{-B\times\Delta t})$ is the time factor that indicates the temporal extension of the contributions of physical transport (A) and biogeochemistry ($\overline{\mathrm{NEB}}$) to the net change of C between 2 consecutive surveys.

Eq. (2) in the case of C_T and A_T should be written as follows:

Table 1. Symbols used throughout the study and their definitions, presented in alphabetical order. Average values determined from data of 2 consecutive surveys

Symbol	Definition
A_T	Total alkalinity (µmol kg^{-1})
C_T	Total inorganic carbon concentration (µmol kg^{-1})
C_L	Average value of variable C in the bottom layer
C_R	Average value of variable C in the river flow
C_U	Average value of variable C in the upper layer
C_S	Average value of variable C in the upper layer of the outer boundary
C_Z	Average value of variable C in the boundary between the upper and lower layers
$\Delta CaCO_3$	Average net ecosystem production (g C m^{-2} d^{-1}) of calcium carbonate
ΔC_{org}	Average net ecosystem production (g C m^{-2} d^{-1}) of organic carbon
$\bar{F}CO_2$	Average air-sea exchange of CO_2 (mmol s^{-1})
$\bar{H}$	Average air-sea exchange of heat (°C m^3 s^{-1})
M_Z	Average vertical turbulent diffusion flux (m^3 s^{-1})
$\overline{NEB}$	Average net ecosystem budget of variable C
pCO_2	Partial pressure of carbon dioxide (µatm)
pCO_2f	pCO_2 (µatm) resulting from advection and diffusion
ΔpCO_2w	pCO_2 (µatm) change due to *in situ* warming
ΔpCO_2org	pCO_2 (µatm) change due to net organic carbon production
ΔpCO_2Ca	pCO_2 (µatm) change due to net calcium carbonate production
$-Q_X$	Offshore Ekman transport (m^3 s^{-1} km^{-1} coast)
Q_B, Q_S	Average bottom and surface horizontal convective water fluxes (m^3 s^{-1}) at the open boundaries of the study area
Q_Z	Average vertical convective water flux (m^3 s^{-1})
Q_R	Average river water flux (m^3 s^{-1})
t_r	Average flushing time (d)
V_U	Average volume (m^3) of the upper layer

$$C_{T_2} = C_{T_1} \times e^{-B(C_T)\times\Delta t} + \left[\frac{A(C_T)}{B(C_T)}\right] \times \left[1 - e^{-B(C_T)\times\Delta t}\right] - \left[\frac{\Delta C_{org} + \Delta CaCO_3}{B(C_T)}\right] \times \left[1 - e^{-B(C_T)\times\Delta t}\right] \quad (3)$$

and

$$A_{T_2} = A_{T_1} \times e^{-B(A_T)\times\Delta t} + \left[\frac{A(A_T)}{B(A_T)}\right] \times \left[1 - e^{-B(A_T)\times\Delta t}\right] + \left[\frac{\frac{16}{106} \times \Delta C_{org} - 2 \times \Delta CaCO_3}{B(A_T)}\right] \times \left[1 - e^{-B(A_T)\times\Delta t}\right] \quad (4)$$

The use of 2 equations (Eqs. 3 & 4) with 2 unknowns (ΔC_{org} and $\Delta CaCO_3$) allows estimation of the net ecosystem production of organic carbon (ΔC_{org}) and calcium carbonate ($\Delta CaCO_3$) in the surface layer of the ría between 2 consecutive surveys. The different values necessary to solve Eqs. (3) & (4) are presented in Table 3. Table 4 shows average values of salinity, temperature, C_T, A_T and pCO_2 for the upper layer of the ría.

Quantification of effects of different factors on seawater pCO_2. The observed pCO_2 of the surface layer of the ría is the result of physical transport of salt, heat, C_T and A_T (pCO_2f), *in situ* warming (ΔpCO_2w), *in situ* net organic carbon production (ΔpCO_2org) and *in situ* net calcification (ΔpCO_2Ca). Over short timescales, the air-sea exchange of CO_2 does not have an important effect on variability of seawater pCO_2 (e.g. Frankignoulle et al. 1996, this study). Air-sea CO_2 exchange within the ría contributes very little to the CO_2 equilibration with the atmosphere due to enhanced flushing rates; the equilibration with the atmosphere takes place in the adjacent shelf, once the water mass has left the ría. The observed pCO_2 can be expressed as:

$$pCO_2 = pCO_2f + \Delta pCO_2w + \Delta pCO_2org + \Delta pCO_2Ca \quad (5)$$

The effect of transport (advection and turbulent diffusion) and *in situ* warming on pCO_2 (pCO_2f + ΔpCO_2w) can be evaluated by calculating C_{T_2} and A_{T_2} with Eqs. (3) & (4) for $\Delta C_{org} = 0$ and $\Delta CaCO_3 = 0$ and then estimating the pCO_2 with the carbonic acid system constants.

ΔpCO_2w was determined by comparing pCO_2f + ΔpCO_2w for the observed temperature of the surface layer with pCO_2f + ΔpCO_2w for the temperature expected if the heat exchange across the sea surface ($\bar{H}$) is set to zero when solving Eq. (2) for temperature.

The effect of *in situ* net calcium carbonate production (ΔpCO_2Ca) was evaluated by comparing pCO_2f + ΔpCO_2w with the pCO_2 resultant from C_{T_2} and A_{T_2} calculated with Eqs. (3) & (4) for $\Delta C_{org} = 0$. (Note that Eqs. 3 & 4 were initially to determine ΔC_{org} and $\Delta CaCO_3$.) In this estimation we used the calculated $\Delta CaCO_3$ and assumed $\Delta C_{org} = 0$ to evaluate C_{T_2} and A_{T_2}. Finally, the effect of *in situ* net organic carbon production (ΔpCO_2org) was evaluated following the same procedure but with $\Delta CaCO_3 = 0$ and the ΔC_{org} initially calculated.

Robustness of estimation of effects of different factors on seawater pCO_2. Inverse methods usually involve the calculation of fluxes and budgets of many different properties with many possible sources of error. In our case, salinity, temperature, C_T and A_T are the properties under consideration and possible errors could arise from (1) convective and diffusive water flows; (2) water, heat and CO_2 air-sea exchange fluxes; (3) representativeness of the salinity, temperature, C_T and A_T determinations at certain sampling stations for

Table 2. Expressions for A and B in Eq. (2), where A/B and B are expected C value in surface layer arising from physical transport and inverse of flushing rate of surface layer, respectively. Situations 1 and 2 correspond to upwelling and downwelling conditions, respectively. See Table 1 for definitions of symbols here and in subsequent tables and in figures

Situation	A	B
1	$\frac{Q_{S1}\times C_{S1} + Q_R\times C_R + Q_Z\times C_Z + \bar{F} + M_Z\times C_L}{V_U}$	$\frac{Q_{S4}\times \frac{<C_{S4}>}{<C>} + M_Z + \frac{dV}{dt}}{V_U}$
2	$\frac{Q_{S1}\times C_{S1} + Q_{S4}\times C_{S4} + Q_R\times C_R + \bar{F} + M_Z\times C_L}{V_U}$	$\frac{Q_Z\times \frac{<C_{S4}>}{<C>} + C_Z + \frac{dV}{dt}}{V_U}$

the average properties of the surface layer; and (4) error transmision in the calculation of pCO_2 from C_T and A_T. According to Matsukawa & Suzuki (1985), the terms and properties involved in these calculations are so numerous that the averaging effect acting on the independent errors is sufficient to decrease the final errors considerably. On this basis, Maamaatuaiahutapu et al. (1992) developed a method based on the random perturbation of the measured variables within the limits of their respective independent error of estimation to asses the robustness of calculations derived from the multiparameter analysis of oceanic water-masses. More recently, Gilcoto et al. (2001) adopted the method for inverse-box methods. In our case, a system of 50 equations for salinity and temperature (Eq. 2), C_T (Eq. 3), and A_T (Eq. 4) were solved for each sampling interval between 2 consecutive surveys. The 50 equations were obtained by random modification of calculated flows and measured variables within the limits of their independent error of estimation. Table 5 shows the error for the estimation of the convective (Q_S, Q_Z) and diffusive (M_Z) water flows provided by Álvarez-Salgado et al. (2000). Despite the fact that the error percentages are larger in spring and autumn than in summer and winter (Table 5), the absolute errors of estimation for the convective fluxes are very similar for the 4 study periods (Álvarez-Salgado et al. 2000). The error of the freshwater flow (Q_R) and the heat-exchange flux ($\bar{H}$) were fixed at 10% according to Álvarez-Salgado et al. (2000). Following Gilcoto et al. (2001), the possible error associated with the sampling strategy was taken into consideration assuming that this represents 20% of the vertical gradient of salinity, temperature, C_T and A_T. The standard deviation of the 50 solutions is the error of the estimation, providing an index of the robustness of the complex calculations performed to separate the different physical and biogeochemical contributions to the observed pCO_2.

Table 6 summarises the error that each flux (Q_S, Q_B, Q_Z, M_Z, Q_R and $\bar{H}$) and property (salinity, temperature, C_T and A_T) produces in the pCO_2 estimation (in µatm)

Table 3. Summary of average water fluxes (Q_{S1}, Q_{S4}, Q_Z, M_Z and Q_R; $m^3\ s^{-1}$), air-sea heat transfer ($\bar{H}$; °C $m^3\ s^{-1}$) and C_T and A_T concentrations (C_{S1}, C_{S4}, C_L, C_U and C_Z; µmol kg^{-1}) for 18 sampling intervals between 2 consecutive surveys performed in the Ría de Vigo during 1997

Date	Q_{S1}	Q_{S4}	Q_Z	M_Z	Q_R	$\bar{H}$	C_T					A_T				
							C_{S1}	C_{S4}	C_L	C_U	C_Z	C_{S1}	C_{S4}	C_L	C_U	C_Z
7–10 Apr	298	−6004	−5885	2259	4.3	1864	2071	2053	2115	2064	2089	2279	2341	2339	2338	2342
10–14 Apr	515	2135	691	2717	6.0	1735	2048	2059	2107	2062	2082	2269	2337	2340	2333	2338
14–17 Apr	257	−73	64	2025	6.7	1638	2015	2055	2112	2058	2083	2271	2335	2345	2329	2337
17–21 Apr	579	−2338	−2608	1561	10.4	346	2045	2039	2107	2049	2078	2264	2328	2337	2322	2335
21–23 Apr	1817	1024	338	2051	16.8	447	2079	2029	2108	2049	2076	2269	2321	2333	2318	2331
1–4 Jul	186	401	861	1184	7.3	1919	1929	2026	2103	2013	2054	2167	2335	2340	2317	2330
4–8 Jul	281	4637	4065	1895	5.4	4234	1938	2034	2102	2020	2056	2190	2339	2341	2326	2336
8–11 Jul	129	−1175	−948	1216	3.2	4710	1915	2041	2094	2029	2052	2198	2341	2345	2331	2337
11–15 Jul	212	5562	4411	2228	2.7	4285	1949	2048	2101	2041	2065	2213	2337	2346	2328	2336
15–18 Jul	212	5933	5874	4690	3.6	6228	2011	2069	2114	2072	2091	2248	2340	2349	2332	2341
15–18 Sep	442	−2295	−1930	2207	2.7	3279	2086	2068	2118	2067	2087	2277	2337	2335	2333	2337
18–22 Sep	404	602	330	1509	2.3	2996	2100	2057	2109	2054	2069	2279	2339	2327	2331	2336
22–25 Sep	269	792	−209	514	2.6	2130	2092	2053	2112	2052	2076	2281	2334	2323	2320	2328
25–29 Sep	216	105	118	1227	4.8	1755	2061	2055	2117	2049	2080	2273	2331	2338	2317	2327
29 Sep–2 Oct	336	−2421	−2242	2433	5.2	1919	2046	2060	2118	2059	2086	2265	2334	2339	2327	2335
1–5 Dec	352	7772	6402	2074	52.2	−3600	1363	2005	2073	1945	2014	1448	2241	2331	2158	2244
5–8 Dec	298	−4478	−1904	3789	42.6	−4027	1694	2027	2066	2009	2035	1835	2278	2325	2258	2281
8–11 Dec	20	−15857	−15276	6769	26.5	−934	1582	1991	2025	1978	1999	1702	2239	2276	2223	2243

Table 4. Summary of the average salinity, temperature (°C), C_T and A_T (µmol kg^{-1}) and pCO_2 (µatm) in the upper layer of the Ría de Vigo during the 22 surveys performed in 1997

Survey	Salinity	Temperature	C_T	A_T	pCO_2
7 Apr	35.7	14.9	2067	2341	325
10 Apr	35.6	15.5	2060	2336	329
14 Apr	35.6	15.9	2063	2330	349
17 Apr	35.6	16.3	2053	2327	342
21 Apr	35.3	16.4	2045	2318	339
23 Apr	35.3	16.2	2052	2319	347
1 Jul	35.5	17.1	2014	2313	308
4 Jul	35.6	16.7	2012	2321	291
8 Jul	35.7	15.8	2028	2333	290
11 Jul	35.6	16.4	2029	2329	303
15 Jul	35.6	15.7	2058	2327	341
18 Jul	35.7	15.3	2085	2336	370
15 Sep	35.7	15.3	2089	2328	392
18 Sep	35.7	15.5	2048	2338	309
22 Sep	35.6	16.0	2059	2324	352
25 Sep	35.6	16.7	2045	2316	350
29 Sep	35.6	16.8	2054	2319	363
2 Oct	35.6	16.9	2065	2334	361
1 Dec	31.3	16.0	1892	2096	359
5 Dec	33.9	16.2	2022	2249	387
8 Dec	34.6	15.7	2003	2262	329
11 Dec	33.7	15.6	1956	2188	348

when the effects of advection + diffusion, warming, net organic carbon production and net calcification are considered separately. Note that the errors produced by Q_R and $\bar{H}$ are quite low (0.2 µatm). Vertical and horizontal advection and mixing as well as the error associated with the representativeness of the property determinations introduce errors of ~3 µatm. ΔC_{org} and $\Delta CaCO_3$ rates for the 4 sampling periods were estimated using Eqs. (3) & (4) with average errors of 17 and 35%, respectively. The errors produced by the introduction of ΔC_{org} and $\Delta CaCO_3$ are ~4 and ~1 µatm, respectively. Finally, note that the random perturbation procedure leads to an average total error of 7.2 µatm, which is much lower than the sum of the independent contribution of each flux and property (13.4 µatm). As pointed out previously, the averaging effect acting on the errors of physical and biogeochemical terms decreases the actual errors considerably.

Table 5. CV (%) in horizontal and vertical convective fluxes during 4 sampling periods (spring, summer, autumn and winter)

Variable	Spring	Summer	Autumn	Winter
Q_Z	44	7	60	8
Q_S, Q_B	15	5	15	7
M_Z	48	13	18	18

RESULTS

Net organic and inorganic carbon production and flushing rates

The hydrographic and meteorological conditions of the Ría de Vigo during 1997 have already been reported in several works (e.g. see Álvarez-Salgado et al. 2000 and Gago et al. 2003 for a detailed description of the space and time evolution of the variables necessary to run the inverse method). The variable that probably best expresses the effect of hydrodynamics on biogeochemistry is flushing time (t_r, d), i.e. the ratio between the volume of the study system and the incoming or outgoing water fluxes. The term $\frac{1}{B} \times (1 - e^{-B \times \Delta t})$, which modulates the effects of net input and the $\overline{NEB}$ of C, is not significantly different from $t_r \times (1 - e^{-\Delta t/t_r})$, the latter being independent of species (salinity, temperature, C_T or A_T). Fig. 2 shows the short-term evolution of t_r and $t_r \times (1 - e^{-\Delta t/t_r})$ for the 4 survey periods. Shelf winds were moderate in intensity and variable in direction during the spring survey. The average offshore Ekman transport for this period was 190 $m^3\ s^{-1}\ km^{-1}$ (Álvarez-Salgado et al. 2000). There was a notable increase in t_r (Fig. 2a), from 2 to more than 6 d, for 7 to 10 April and 14 to 17 April, respectively. The term $t_r \times (1 - e^{-\Delta t/t_r})$ ranged from 1.5 to 2.5 d. The summer period coincided with northerly winds that produced intense offshore Ekman transport values: the average transport was 365 $m^3\ s^{-1}\ km^{-1}$. In contrast, continental runoff was extremely low at <7 $m^3\ s^{-1}$. A decrease of t_r from the beginning to the end of the

Table 6. Average error in estimation of calculated pCO_2 (µatm), standard deviation of 50 solutions, due to errors in river flow and heat-exchange flux (Q_R, $\bar{H}$, respectively), vertical advection (Q_Z), horizontal advection (Q_S, Q_B), vertical mixing (M_Z) and representativeness of property concentrations (salinity, temperature, A_T and C_T)

Variable	Advection	Heat	ΔC_{org}	$\Delta CaCO_3$	Net error
Q_R, $\bar{H}$	0.3	0.2	~0	~0	0.2
Q_Z	2.8	0.1	0.1	~0	2.8
Q_S, Q_B	1.6	0.1	0.4	0.1	1.7
M_Z	2.9	0.1	0.1	~0	3.0
S, T, A_T, C_T	2.8	~0	4.4	1.3	5.7
Total	4.8	0.2	4.3	1.4	7.2

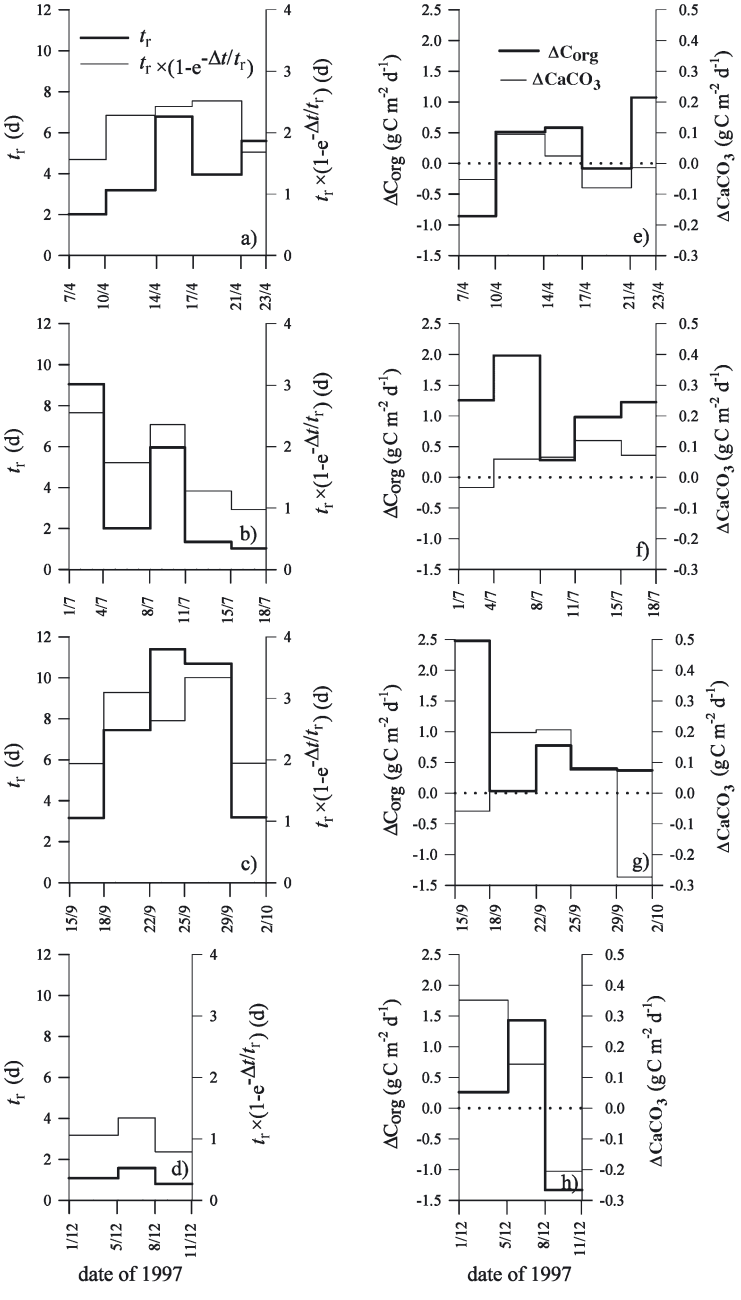

Fig. 2. Temporal evolution of (left panels) t_r and $t_r \times (1 - e^{-\Delta t/t_r})$ and of (right panels) net ecosystem production of organic carbon (ΔC_{org}) and calcium carbonate ($\Delta CaCO_3$) during (a,e) spring, (b,f) summer, (c,g) autumn and (d,h) winter survey periods of 1997. Dates given as d/mo

summer survey was observed (Fig. 2b) due to upwelling intensification during this period. At the end of the summer period, strong upwelling reduced flushing time to 1 d. A prolonged (>10 d) wind calm—characteristic of the transition from the upwelling to the downwelling season (Álvarez-Salgado et al. 2000)—was monitored during the autumn period. The offshore Ekman transport ranged from –30 to 160 m^3 s^{-1} km^{-1}, with an average value of 109 m^3 s^{-1} km^{-1}, and the continental runoff was again quite limited: <5 m^3 s^{-1}, with t_r and $t_r \times (1 - e^{-\Delta t/t_r})$ reaching maximum values (always more than 4 and 3 d, respectively (Fig. 2c). Dramatic changes in the wind regime occurred during the winter (1 to 11 December), evolving from upwelling-favorable northerly winds producing an offshore Ekman transport of 200 m^3 s^{-1} km^{-1} on 1 to 5 December to downwelling-favorable southerly winds producing an offshore Ekman transport of –1500 m^3 s^{-1} km^{-1} on 8 to 12 December. Continental runoff was very high during the winter period (average 40 m^3 s^{-1}). t_r and $t_r \times (1 - e^{-\Delta t/t_r})$ remained approximately constant at 1 d as a result of the intensified circulation (Fig. 2d).

The net ecosystem production of organic carbon (ΔC_{org}) and of calcium carbonate ($\Delta CaCO_3$) in the upper layer of the Ría during the 4 survey periods is also presented in Fig. 2. $\Delta CaCO_3$ was very low during the 4 periods, being slightly intensified in the autumn surveys (18 to 25 September average, 0.2 g C m^{-2} d^{-1}). An increase in ΔC_{org} from the beginning to the end of the period was observed during spring (Fig. 2e), parallel to the temporal evolution of t_r. In the period 7 to 10 April, negative ΔC_{org} values were observed (ΔC_{org} = –0.86 g C m^{-2} d^{-1}), denoting the dominance of respiration processes. At the beginning of the summer (Fig. 2f), the highest ΔC_{org} for this period was observed (4 to 8 July = 2 g C m^{-2} d^{-1}). In contrast, strong upwelling occurred at the end of this period (the lowest t_r was observed) and ΔC_{org} was reduced. The highest ΔC_{org} was found on 15 to 18 September (2.5 g C m^{-2} d^{-1}: Fig. 2g), as a result of favorable physical and biological conditions. It is known that upwelling systems achieve maximum productivity during moderate wind conditions when longer flushing times allow phytoplankton to adapt to the new light and nutrient conditions (Wroblewski & Hoffmann 1989). ΔC_{org} rates during the other surveys in September fluctuated between 0.0 and 0.8 g C m^{-2} d^{-1}. The high values of t_r and $t_r \times (1 - e^{-\Delta t/t_r})$ resulted in an intense effect of the $\overline{NEB}$ and A (ratio of the C input to the system divided by the volume of the reservoir) on the final concentration of C. Finally, the winter period was characterized by strong changes in ΔC_{org} (Fig. 2h): from a production of 1.4 g C m^{-2} d^{-1} during 5 to 8 December to a respiration of –1.3 g C m^{-2} d^{-1} during 8 to 11 December. The pronounced ΔC_{org} minimum at the end of the winter period coincided with remarkably negative values of $-Q_X$.

Physical and biogeochemical components of surface pCO_2 variability

Fig. 3 shows the short-term evolution of observed pCO_2 (see Table 4), the pCO_2 expected if only advection and turbulent diffusion of carbon species occur (pCO_2f) and the pCO_2 expected if *in situ* warming due to heat exchange with the atmosphere is also considered ($pCO_2f + \Delta pCO_2w$). During spring, the observed pCO_2 increased from 325 to 345 µatm (Fig. 3a). As a consequence of the net respiration during 7 to 10 April, pCO_2f was slightly lower than observed pCO_2. The most intense effect of *in situ* warming on pCO_2 was observed during 10 to 17 April, being almost nil on the other dates in April. During the summer period, pCO_2 (Fig. 3b) showed a time evolution inverse to t_r (Fig. 2b), with a steep increase from 290 µatm on 4 July to 370 µatm on 18 July. This pCO_2 increase resulted from upwelling intensification. pCO_2f was always higher than the observed pCO_2. Biological activity had an important effect on pCO_2 during 1 to 7 July. Thereafter, the modulating effect of ΔC_{org} on pCO_2 was weakened as a result of reduced flushing times. Warming was more important in this period than during April, due to enhanced irradiance. The highest $pCO_2f + \Delta pCO_2w$ value of the 4 periods studied was reached on 18 July. This resulted from the combined effect of upwelling and warming on pCO_2.

During the autumn surveys (Fig. 3c), the large ΔC_{org} observed between 15 and 18 September had a dramatic effect on pCO_2, which was reduced by almost 70 µatm compared with pCO_2f. On the other dates, pCO_2 values ranged from 350 to 360 µatm, very close to the mean atmospheric value for 1997 (365 µatm) according to Gago et al. (2003). pCO_2f exhibited the lowest variability of the 4 periods and the effect of warming on pCO_2 was nearly constant at approximately +5 µatm. During the winter, pCO_2 values ranged from 387 µatm on 5 December to 329 µatm on 8 December (Fig. 3d). As a result of the strong upwelling event at the beginning of this period, pCO_2f during 1 to 5 December was the highest of all survey periods (400 µatm). In this case, a net transfer of heat from the sea to the atmosphere provoked a net decrease of 6 µatm in $pCO_2f + \Delta pCO_2w$ compared with pCO_2f. The effect of cooling was negligible during 8 to 11 December. Net respiration during 8 to 11 December provoked an important increase of the observed pCO_2 compared with pCO_2f.

Fig. 3 also shows the net effect of *in situ* warming, *in situ* ΔC_{org} and *in situ* $\Delta CaCO_3$ on the observed pCO_2, taking pCO_2f as a reference value. Net *in situ* calcification had no important effect on pCO_2, with average values ranging from 0 to 2 µatm in April and December, respectively. Air-sea heat exchange was positive during the periods of April, July and September. Therefore there was a thermodynamic increase of pCO_2 due to surface heating. The average value during July was the highest, 8 µatm (Fig. 3f). In December there was a cooling of the surface layer of the ría, and

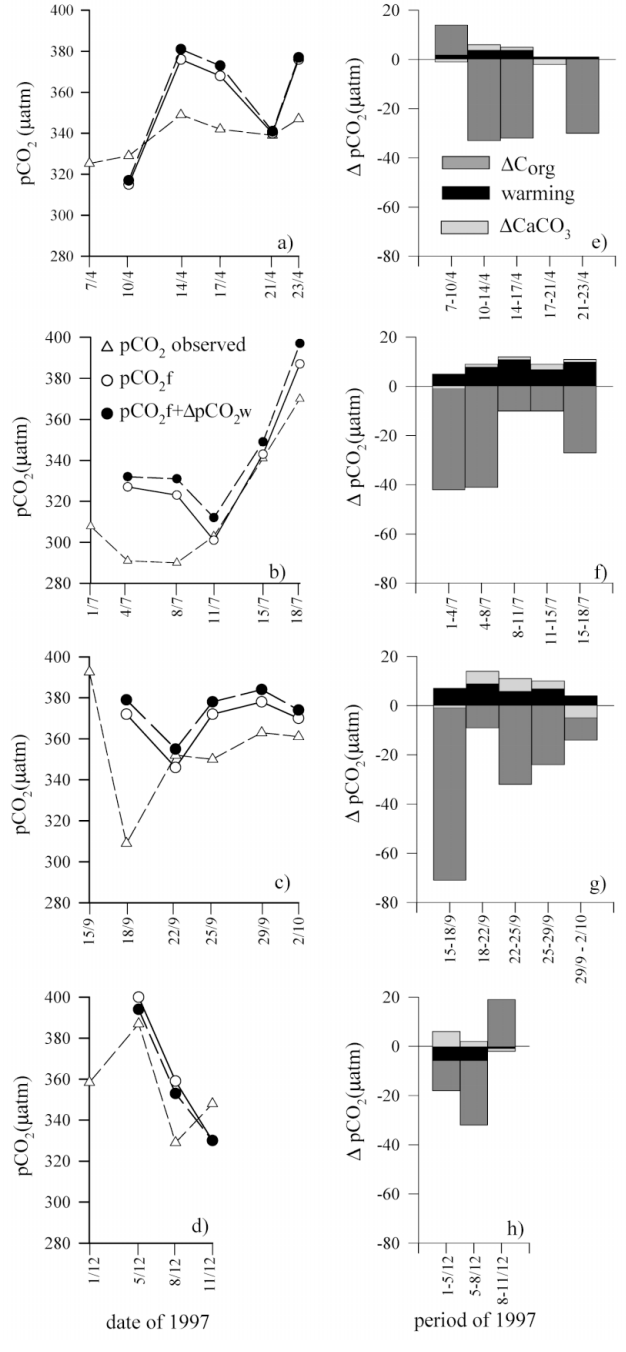

Fig. 3. Temporal evolution of (left panels) pCO_2, pCO_2f and $pCO_2f + \Delta pCO_2w$ and of (right panels) the net effect on pCO_2 of warming and net ecosystem production of organic carbon (ΔC_{org}) and calcium carbonate ($\Delta CaCO_3$) during (a,e) spring, (b,f) summer, (c,g) autumn and (d,h) winter survey periods of 1997. Dates given as d/mo

Table 7. Summary of significant regression between pCO_2, pCO_2f, ΔpCO_2w, ΔpCO_2org and ΔpCO_2Ca (n = 18 in all cases; the origin intercept is not significant in all cases, $p > 0.1$)

Case	Statistical results
pCO_2 vs pCO_2f	$r^2 = 0.53$; $p < 0.001$
pCO_2 vs $pCO_2f + \Delta pCO_2w$	$r^2 = 0.48$; $p < 0.001$
pCO_2 vs $pCO_2f + \Delta pCO_2Ca$	$r^2 = 0.54$; $p < 0.001$
pCO_2 vs $pCO_2f + \Delta pCO_2org$	$r^2 = 0.96$; $p < 0.001$

this provoked an average decrease of 4 µatm in the observed pCO_2 (Fig. 3h) compared with pCO_2f. In all cases, ΔC_{org} was the most important process affecting ΔpCO_2. The highest average effects of ΔC_{org} occurred during July and September: –26 and –29 µatm, respectively. As indicated above, the highest decrease, 70 µatm, was observed between 15 and 18 September.

The linear correlations between observed pCO_2 and the different contributions (physical transport, *in situ* warming, *in situ* net organic carbon production and *in situ* calcification) are summarized in Table 7. It should be stressed that the advection + turbulence diffusion term explained nearly 50% of the observed variance and the ΔC_{org} term contributed the remaining 50%. The other terms, warming and calcification, had almost no effect on the correlations. When included, the term *in situ* calcification marginally improved the correlation. Fig. 4 shows observed pCO_2, pCO_2f, $pCO_2f + \Delta pCO_2org$ and the 1:1 line for the 18 periods between 2 consecutive surveys sampled during 1997. As can be seen, the $pCO_2f + \Delta pCO_2org$ term was almost identical to the observed pCO_2 values.

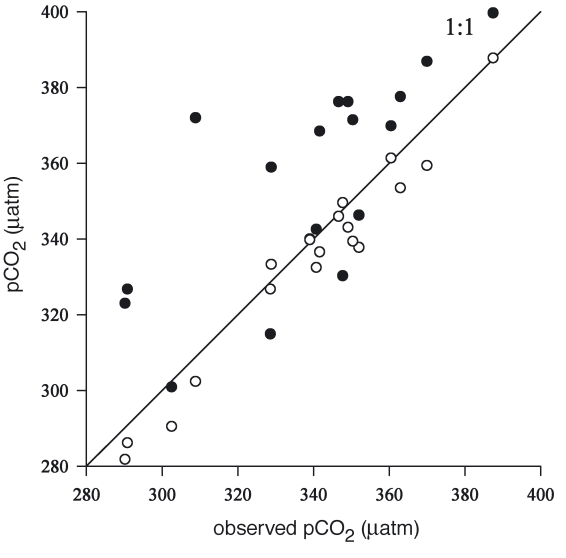

Fig. 4. Observed pCO_2 versus pCO_2f (●) and $pCO_2f + \Delta pCO_2org$ (○). The 1:1 line is shown

DISCUSSION AND CONCLUSIONS

According to previous studies, pCO_2 transient undersaturation generally exists in surface waters of the Spanish Rías Baixas under conditions of moderate upwelling as a result of intense inorganic carbon uptake by phytoplankton. In contrast, pCO_2 transient oversaturation occurred during strong upwelling events (Álvarez et al. 1999, Rosón et al. 1999, Gago et al. 2003) due to strong upwelling of aged pCO_2-rich Eastern North Atlantic Central Water (ENACW). During downwelling events, pCO_2-undersaturated oceanic surface waters penetrate into the rías (Pérez et al. 1999, Borges & Frankignoulle 2002).

Despite the fact that box models have been extensively used for studies of pollutant dispersal, carbon and nutrient biogeochemistry, or phytoplankton dynamics in estuaries and coastal embayments (e.g. Downing 1971, Chang & Carpenter 1985, Pérez et al. 2000), they have never been used to study the short-term variability of surface pCO_2. In this work, we present a reliable method for objectively quantifying the net effect of physical (advection and diffusion of inorganic carbon species, *in situ* warming) and biogeochemical (production and consumption of inorganic carbon species) processes on the observed surface pCO_2 that is suitable for estuaries and coastal inlets with only 1 open boundary (although it could easily be adapted to more complex coastal systems). In general, the net effect of carbon biogeochemistry upon surface pCO_2 depends on the intensity of the processes involved (ΔC_{org} and $\Delta CaCO_3$) and the time period (t_r). Therefore, the effect of carbon biogeochemistry on surface pCO_2 is (1) determined (transport of aged pCO_2 and nutrient-rich subsurface ocean waters) and (2) modulated (flushing time) by the physical conditions of coastal upwelling systems. These general (and expected) conclusions are discussed below.

Compared with other coastal upwelling systems, 2 conspicuous characteristics of the NW Iberian shelf should be considered: (1) The coast of NW Spain lies within the North Atlantic ventilated thermocline (Castro et al. 2000), and therefore nutrient and pCO_2 levels of the upwelled ENACW are much lower than in the central waters of the South Atlantic (which upwell along the Namibia-Benguela coastline), South Pacific waters (which upwell along the Perú-Chile coastline) and those of the North Pacific (which upwell along the California-Oregon coastline). As an example, phosphate and pCO_2 levels of upwelled ENACW in NW Spain rarely exceed 1.0 µM and 450 µatm, respectively (Castro et al. 2000), whereas subsurface waters off Perú can exceed 2 µM and 1000 µatm, respectively (Copin-Montegut & Raimbault 1994). (2) Coastal winds off NW Spain are very variable, following successive

stress-relaxation cycles with a periodicity of between 5 and 15 d (Álvarez-Salgado et al. 1993); this allows efficient utilization of upwelled nutrients during the relaxation events because of enlarged flushing times that lead to pCO_2 undersaturation.

Our ΔC_{org} (net ecosystem production of organic carbon) estimates for the Ría de Vigo exceed the average annual net primary production of the global coastal zone (0.14 to 0.33 g C m^{-2} d^{-1}; Wollast 1993) and are similar to the annual mean of gross primary production proposed by Boynton et al. (1982) for coastal upwelling areas (0.82 g C m^{-2} d^{-1}). In support of our results, Moncoiffé et al. (2000), using the oxygen incubation method, reported an average net primary production rate in the central Ría de Vigo of 0.7 to 0.9 g C m^{-2} d^{-1} during the upwelling season of 1991. The extreme short-term variability of net organic carbon production rates in our study is in accordance with the results of Tilstone et al. (1999), Moncoiffé et al. (2000) and Pérez et al. (2000). These relatively high and very variable ΔC_{org} values themselves explain ~50% of the short-term (2 to 4 d) variability in surface pCO_2 and are responsible for the pCO_2 undersaturation normally observed in the Ría de Vigo despite reduced flushing times and elevation of pCO_2-rich ENACW during upwelling events.

Our $\Delta CaCO_3$ (net ecosystem production of calcium carbonate) estimates for the Ría de Vigo, with average values ranging from 0.07 to 0.22 g C m^{-2} d^{-1}, are in agreement with those obtained by Rosón et al. (1999) for the adjacent Ría de Arousa. Coccolithophore blooms and coral reefs are commonly considered as being primarily responsible for calcification in the marine environment. Robertson et al. (1994) determined a mean increase in pCO_2 of 15 µatm due to the effect of calcification during a Northeast Atlantic coccolithophore bloom in the spring of 1991, while Frankignoulle et al. (1996) estimated that the effect of coral reefs on surface pCO_2 in French Polynesia is negligible on a daily scale. The latitude and the hydrographic regime of the NW Iberian upwelling system do not allow development of either coccolithophore blooms (e.g. Figueiras & Ríos 1993) or corals. However, another conspicuous characteristic of the Spanish Rías Baixas should not be forgotten: they support the most intensive mussel cultures in the world (Tenore et al. 1982), representing 40% of the European and 20% of the world production in 1997 (Labarta 2000). The culture of mussels on hanging ropes in the Ría de Vigo produced ~5×10^7 kg wet weight in 1997. Since mussel shelves represent ~50% of the wet weight of commercial mussels and ~90% of the shelves are comprised of $CaCO_3$ (Rosón et al. 1999), the mussels of the Ría de Vigo would have produced an average of ~0.06 g C m^{-2} d^{-1} of $CaCO_3$ during 1997. This is reflected in our low $\Delta CaCO_3$ estimates. The effect of calcification on surface pCO_2 variability in the Ría de Vigo is less than 5 µatm.

With regard to the effect of *in situ* warming of the surface layer of the Ría de Vigo through heat exchange across the sea surface, pCO_2 ranges from −6 to +11 µatm at *in situ* warming values from −0.4 to +0.8°C respectively. This is again negligible compared with the effects of circulation and ΔC_{org}. The effect of *in situ* warming is probably more pronounced in coastal upwelling systems at lower latitudes than NW Spain (40 to 43° N), e.g. along Namibia-Benguela and Perú (<35° S) coastlines and in Southern California (<35° N), because of enhanced solar irradiation. *In situ* warming would also be important in upwelling systems in which the upwelled central waters are colder than off NW Spain (12 to 14°C), e.g. Oregon (8 to 10°C), because of enhanced heat exchange across the sea surface.

In this study, we have separated the effects of advection + diffusion, air-sea heat exchange, net organic carbon production and calcification on surface pCO_2 variability of a coastal upwelling system. The coupling of physical and biological processes — upwelling of cool aged subsurface ocean waters to the photic layer of the coastal ecosystem, where they undergo heating and promote intensified primary production rates — has been extensively described in the literature, but no studies have determined quantitatively the net effect of these processes on surface pCO_2 dynamics on a short time-scale. Using a simple box model, Louanchi et al. (1999) found that biological activity can contribute up to 45% of sea-surface pCO_2 variability in the Southern Ocean on a monthly scale. Sabine & Key (1998) applied a process analysis to CO_2 data for the Southern Ocean and determined that pCO_2 variability is strongly dependent on biological as well as physical processes. This methodology was applied to the Ría de Vigo by Álvarez et al. (1999), who showed that organic matter production explains almost 60% of the pCO_2 variability on a monthly scale. Our quantitative approach has shown for the first time that contributions of physical and biogeochemical factors to surface pCO_2 variability on a half-weekly scale are of the same order in highly dynamic coastal upwelling systems such as the Ría de Vigo.

Acknowledgements. The authors wish to thank the captain and crew of RV 'Mytilus', and the members of the IIM Group of Oceanography for their assistance during the sampling program. Special thanks to B. Míguez for the elaboration of the FORTRAN program to calculate average thermohaline and chemical properties. Financial support for this work came from the Spanish 'Comisión Interministerial de Ciencia y Tecnología' (CICYT), Grant No. AMB95–1084. A fellowship from the Spanish 'Ministerio de Educación y Ciencia' funded J. G. during this work.

LITERATURE CITED

Álvarez M, Fernández E, Pérez FF (1999) Air-sea CO_2 fluxes in a coastal embayment affected by upwelling: physical versus biological control. Oceanol Acta 22:499–515

Álvarez-Salgado XA, Rosón G, Pérez FF, Pazos Y (1993) Hydrographic variability off the Rías Baixas (NW Spain) during the upwelling season. J Geophys Res 98: 14447–14455

Álvarez-Salgado XA, Gago J, Míguez BM, Gilcoto M, Pérez FF (2000) Surface waters of the NW Iberian margin: upwelling on the shelf versus outwelling of upwelled waters from the Rías Baixas. Estuar Coast Shelf Sci 51: 821–837

Borges AV, Frankignoulle M (2002) Aspects of dissolved inorganic carbon dynamics in the upwelling system off the Galician coast. J Mar Sys 32:181–198

Boynton WR, Kemp WM, Keefe CW (1982) A comparative analysis of nutrients and other factors influencing estuarine phytoplankton productions. In: Kennedy VS (ed) Estuarine comparisons. Academic Press, New York, p 69–90

Broecker WS, Peng TH (1982) Tracers in the sea. Eldigio Press, New York

Castro CG, Pérez FF, Álvarez-Salgado XA, Fraga F (2000) Coupling between the thermohaline, chemical and biological fields during 2 contrasting upwelling events off the NW Iberian Peninsula. Cont Shelf Res 20:189–210

Chang J, Carpenter EJ (1985) Blooms of the dinoflagellate *Gyrodinyum aureolum* in a Long Island estuary: box model analysis of bloom maintenance. Mar Biol 89:83–93

Copin-Montegut C, Raimbault P (1994) The Peruvian upwelling near 15° S in August 1986. Results of continuous measurements of physical and chemical properties between 0 and 200 m depth. Deep-Sea Res Part I 41: 439–467

Downing AL (1971) Forecasting the effects of polluting discharges on natural waters. II. Estuaries and coastal waters. Int J Environ Stud 2:221–226

Figueiras FG, Ríos AF (1993) Phytoplankton succession, red tides and the hydrographic regime in the Rías Bajas of Galicia. In: Smayda TJ, Shimizu Y (eds) Toxic phytoplankton blooms in the sea. Elsevier, Amsterdam, p 239–244

Frankignoulle M, Gatusso JP, Biondo R, Bourge I, Copin-Montegut G, Pichon M (1996) Carbon fluxes in coral reefs. II. Eulerian study of inorganic carbon dynamics and measurement of air-sea CO_2 exchanges. Mar Ecol Prog Ser 145:123–132

Gago J, Gilcoto M, Pérez FF, Ríos AF (2003) Short-term variability of fCO_2 in seawater and air-sea CO_2 fluxes in a coastal upwelling system (Ría de Vigo, NW Spain). Mar Chem 80:247–264

Gilcoto M, Álvarez-Salgado XA, Pérez FF (2001) Computing optimum estuarine residual fluxes with (OERFIM) a multiparameter inverse method: application to the Ría de Vigo (NW Spain). J Geophys Res 106:31303–31318

Houghton JT, Meira Filho LG, Callander BA, Harris N, Kattenberg A, Maskell K (1996) Climate change 1995: the science of climate change. Cambridge University Press, Cambridge

Knauer GA (1993) Interactions of carbon and nitrogen cycles in the coastal zone. In: Wollast R, Mackenzie FT, Chou L (eds) Interactions of C, N, P and S biogeochemical cycles and global change. Springer-Verlag, Heidelberg, p 210–231

Komhyr WD, Gammon RH, Harris TB, Waterman LS, Conway TJ, Taylor WR, Thoning KW (1985) Global atmospheric CO_2 distribution and variations from 1968–1982. NOAA/GMCC CO_2 flask sample data. J Geophys Res 90: 5567–5596

Labarta U (2000) Desarrollo e innovación empresarial en la acuicultura: una perspectiva gallega en un contexto internacionalizado. Fundación CaixaGalicia, A Coruña (Doc Econ 6)

Louanchi F, Ruiz-Pino DP, Poisson A (1999) Temporal variations of mixed-layer oceanic CO_2 at JGOFS-KERFIX time-series station: physical versus biogeochemical processes. J Mar Res 57:165–187

Maamaatuaiahutapu K, Garçon VC, Provost C, Boulahdid M, Osiroff AP (1992) Brazil-Malvinas confluence: water mass composition. J Geophys Res 97:9493–9505

Martin JM, Mouchel JM, Thomas AJ (1986) Time concepts in hydrodynamic systems with an application to ^{7}Be in the Gironde estuary. Mar Chem 18:369–392

Matsukawa Y, Suzuki T (1985) Box model analysis of hydrographic behaviour of nitrogen and phosphorus in a eutrophic estuary. J Oceanogr Soc Japan 41:407–426

Mehrbach C, Culberson CH, Hawley JE, Pytkowicz RM (1973) Measurement of the apparent dissociation constants of carbonic acid in seawater at atmospheric pressure. Limnol Oceanogr 18:897–907

Moncoiffé G, Álvarez-Salgado XA, Figueiras FG, Savidge G (2000) Seasonal and short-time-scale dynamics of microplankton community production and respiration in an inshore upwelling system. Mar Ecol Prog Ser 196:111–126

Pérez FF, Fraga F (1987a) The pH measurements in seawater on the NBS scale. Mar Chem 21:315–327

Pérez FF, Fraga F (1987b) A precise and rapid analytical procedure for alkalinity determination. Mar Chem 21: 169–182

Pérez FF, Ríos AF, Rosón G (1999) Sea surface carbon dioxide off the Iberian Peninsula (North Eastern Atlantic Ocean). J Mar Syst 19:27–46

Pérez FF, Álvarez-Salgado XA, Rosón G (2000) Stoichiometry of the net ecosystem metabolism in a coastal inlet affected by upwelling. The Ría de Arousa (NW Spain). Mar Chem 69:217–236

Ríos AF, Nombela MA, Pérez FF, Rosón G, Fraga F (1992) Calculation of runoff to an estuary, Ría de Vigo. Sci Mar 53:29–33

Robertson JE, Robinson C, Turner DR, Holligan P, Watson AJ, Boyd P, Fernández E, Finch M (1994) The impact of a coccolithophore bloom on oceanic carbon uptake in the Northeast Atlantic during summer 1991. Deep-Sea Res Part I 2:297–314

Rosón G, Álvarez-Salgado XA, Pérez FF (1999) Carbon cycling in a large coastal embayment, affected by wind-driven upwelling: short-time-scale variability and spatial differences. Mar Ecol Prog Ser 176:215–230

Sabine CL, Key RM (1998) Controls of fCO_2 in the South Pacific. Mar Chem 60:95–110

Schimel D, Enting AI, Heiman M, Joos F, Raynaud D, Wigley T (1995) CO_2 and the carbon cycle. In: Houghton JT, Meira Filho LG, Callender BA, Harris N, Kattenberg A, Maskell K (eds) Climate change 1995. Cambridge University Press, Cambridge, p 76–86

Siegenthaler U, Sarmiento JL (1993) Atmospheric carbon dioxide and the ocean. Nature 365:119–125

Takahashi T, Olafsson J, Goddard JG, Chipman DW, Sutherland SC (1993) Seasonal variation of CO_2 and nutrients in the high-latitude surface oceans: a comparative study. Global Biogeochem Cycles 7:843–878

Tenore KR, Boyer LF, Cal RM, García Fernández C and 14 others (1982) Coastal upwelling in the Rías Bajas, NW Spain: contrasting the benthic regimes in the Rías of Arosa and Muros. J Mar Res 40:701–720

Tilstone GH, Figueiras FG, Fermín EG, Arbones B (1999)

Significance of nanophytoplankton photosynthesis and primary production in a coastal upwelling system (Ría de Vigo, NW Spain). Mar Ecol Prog Ser 183:13–27

Torres R, Turner DR, Silva N, Rutllant J (1999) High short-term variability of CO_2 fluxes during an upwelling event off the Chilean coast at 30° S. Deep-Sea Res Part I 46: 1161–1179

UNESCO (1986) The international system of units (SI) in oceanography. UNESCO Tech Pap Mar Sci 50:13–17

Walsh JJ (1991) Importance of continental margins in the marine biogeochemical cycling of carbon and nitrogen. Nature 359:53–55

Watson AJ (1995) Are upwelling zones sources or sinks of CO_2? In: Summerhayes CP, Emeis KC, Angel MV, Smith RL, Zeitzschel B (eds) Upwelling in the ocean. Modern processes and ancient records. John Wiley & Sons, Chichester, p 321–336

Weiss RF (1974) Carbon dioxide in water and seawater: the solubility of a non ideal gas. Mar Chem 2:203–215

Wollast R (1993) Interactions of carbon and nitrogen cycles in the coastal zone. In: Wollast R, Mackenzie FT, Chou L (eds) Interactions of C, N, P and S biogeochemical cycles and global change. Springer-Verlag, Heidelberg, p 195–210

Wooster WS, Bakun A, McClain DR (1976) The seasonal upwelling cycle along the eastern boundary of the North Atlantic. J Mar Res 34:131–141

Wroblewski JS, Hoffmann EE (1989) US interdisciplinary modelling studies of coastal-offshore exchange processes: past and future. Prog Oceanogr 23:65–69

Editorial responsibility: Otto Kinne (Editor), Oldendorf/Luhe, Germany

Submitted: October 29, 2002; Accepted: April 10, 2003
Proofs received from author(s): June 11, 2003